

Dalton Transactions

Accepted Manuscript



This is an *Accepted Manuscript*, which has been through the Royal Society of Chemistry peer review process and has been accepted for publication.

Accepted Manuscripts are published online shortly after acceptance, before technical editing, formatting and proof reading. Using this free service, authors can make their results available to the community, in citable form, before we publish the edited article. We will replace this *Accepted Manuscript* with the edited and formatted *Advance Article* as soon as it is available.

You can find more information about *Accepted Manuscripts* in the [Information for Authors](#).

Please note that technical editing may introduce minor changes to the text and/or graphics, which may alter content. The journal's standard [Terms & Conditions](#) and the [Ethical guidelines](#) still apply. In no event shall the Royal Society of Chemistry be held responsible for any errors or omissions in this *Accepted Manuscript* or any consequences arising from the use of any information it contains.

ARTICLE

Rapid microwave-assisted synthesis of a sodium-cadmium metal-organic framework having improved performance as CO₂ adsorbent for CCS

Cite this: DOI: 10.1039/x0xx00000x

Carlos Palomino Cabello,^a Carlos Otero Arean,^a José B. Parra,^b Conchi O. Ania,^b P. Rumori,^a and G. Turnes Palomino^{a,*}

Received 00th January 2012,
Accepted 00th January 2012

DOI: 10.1039/x0xx00000x

www.rsc.org/

^a Department of Chemistry, University of the Balearic Islands, 07122 Palma de Mallorca, Spain. Tel.: (+34)-971-173250; Fax: (+34)-971-173426; E-mail: g.turnes@uib.es

^b Instituto Nacional del Carbón, INCAR-CSIC, Apdo. 73, 33080 Oviedo, Spain

We report on a facile and rapid microwave-assisted method for preparing a sodium-cadmium metal-organic framework (having coordinatively unsaturated sodium ions) that considerably shortens the conventional synthesis time from 5 days to 1 hour. The obtained (Na,Cd)-MOF showed an excellent volumetric CO₂ adsorption capacity (5.2 mmol cm⁻³ at 298 K and 1 bar) and better CO₂ adsorption properties than those shown by the same metal-organic framework when synthesized following a more conventional procedure. Moreover, the newly prepared material was found to display high selectivity for adsorption of carbon dioxide over nitrogen, and good regenerability and stability during repeated CO₂ adsorption-desorption cycles, which are required properties for any adsorbent intended for carbon dioxide capture and sequestration (CSS) from the post-combustion flue gas of fossil fuelled power stations.

Introduction

The rising of carbon dioxide emissions from anthropogenic sources, with consequent increase of greenhouse effect, is of worldwide environmental concern nowadays. Power plants that burn fossil fuels to produce electricity constitute a main source of CO₂ emission to the atmosphere, and demand of that energy is likely to keep increasing in the future mainly because of economic growth and increased industrialization, especially in developing countries.^{1,2} Replacing fossil fuels with renewable, and cleaner, energy sources could provide a way out of this problem in the long run, but, in the interim, finding a way to continue using fossil fuels while curbing carbon dioxide emissions would be highly desirable.³ In this context, it is worthwhile pointing out that estimations from the Intergovernmental Panel on Climate Change (IPCC) have shown that CO₂ emissions could be very significantly reduced in modern power plants equipped with suitable carbon dioxide capture and storage (CSS) technology.^{4,5}

Metal-organic frameworks (MOFs) are among the porous solids currently more widely investigated as potential candidates for carbon dioxide capture by physical adsorption, as testified by the considerable number of recent reviews dealing with that subject.^{2,4,6-11} MOFs are prepared by joining metal cations (or cationic clusters) with organic linkers, which results in a large variety of chemical composition and structure types, most of them showing permanent porosity and large internal surface area, which favour high gas uptake by physisorption. The large number of structures that can be obtained by changing either the organic linker or the metal

cation endows MOFs with a high versatility for tuning chemical composition, pore size and surface area, and hence reversible gas adsorption properties. However, in contrast to the large number of MOFs containing transition metal ions reported in the literature, examples based on alkaline or alkaline earth metals are so far scarce;^{12,13} and among them, only a few have demonstrated to be capable of gas sorption until now. Recently, the use of s-block metal cations in the design and preparation of metal-organic frameworks has been reviewed by Banerjee and Parise.¹² According to these authors, the dominance of ionic forces in this kind of MOFs renders their synthesis rather difficult, and the lack of preformed secondary building units often leads to low dimensional networks. Nevertheless, that can be avoided by simultaneous incorporation of s-block elements and other metal centres, which can lead to tridimensional heterobimetallic MOFs containing the desired alkaline (or alkaline-earth) metal cation.¹² Following this approach, Fu et al.¹⁴ have recently reported the synthesis of a novel sodium-cadmium organic framework having narrow channels, and which shows permanent porosity. This sodium-cadmium MOF has the composition [Cd₃Na₆(BTC)₄(H₂O)₁₂]·H₂O, crystallizes in the tetragonal space group P4₂/n (because complex connection between structural units lowers the otherwise cubic symmetry, P $\bar{4}$ 3m), and shows a tridimensional structure formed by two interpenetrated [Cd₃(BTC)₄] open frameworks bridged together by {Na₃O₁₂} trimmers (Fig. 1).¹⁴ The resulting structure displays a 3D pore system formed by mutually intersecting (approximately cylindrical) channels running in three directions. In the as-synthesized material

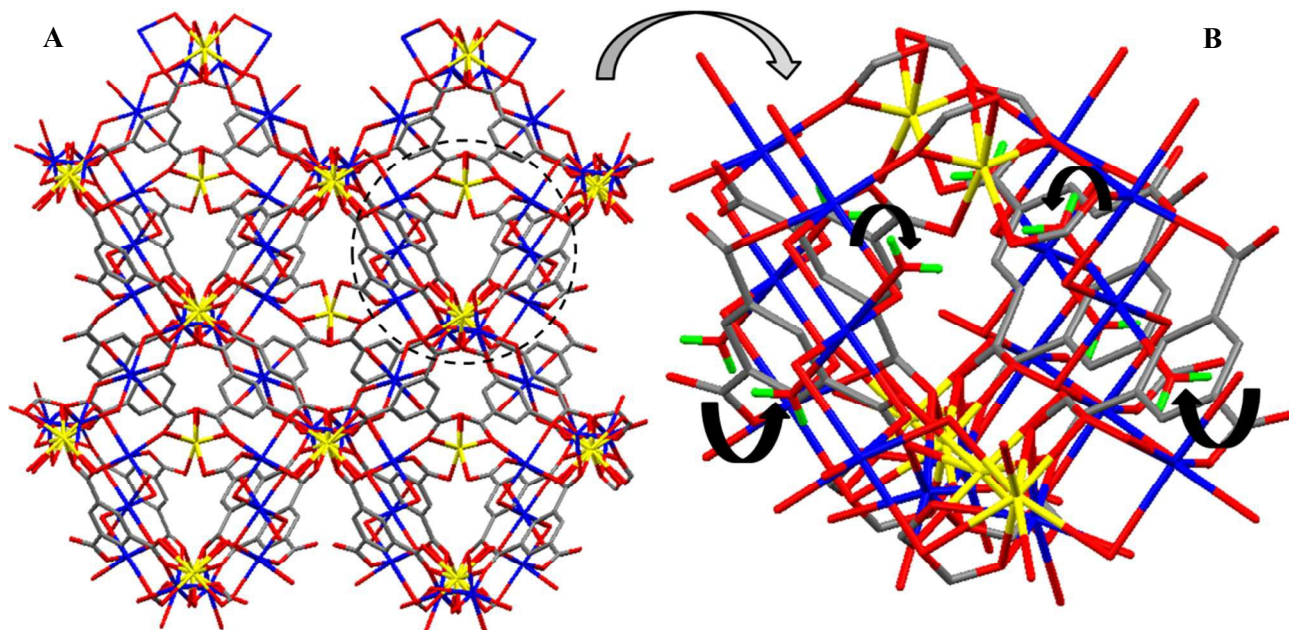


Fig. 1 A) View of the structure of the sodium-cadmium metal-organic framework $[\text{Cd}_3\text{Na}_6(\text{BTC})_4(\text{H}_2\text{O})_{12}]\cdot\text{H}_2\text{O}$. B) Detail showing the coordination of labile water molecules to sodium ions. Sodium, cadmium, carbon and oxygen atoms are shown in blue, yellow, gray and red, respectively; hydrogen atoms of removable water molecules in green (adapted from ref. 14).

sodium cations have labile water molecules in their coordination sphere that can be removed, by appropriate thermal treatment and outgassing, to leave coordinatively unsaturated Na^+ sites, which can act as gas adsorption centres. The cadmium cations, however, are fully coordinated to the organic linkers of the MOF framework. More details on the $[\text{Cd}_3\text{Na}_6(\text{BTC})_4(\text{H}_2\text{O})_{12}]\cdot\text{H}_2\text{O}$ structure can be found elsewhere.¹⁴

Typically, MOFs are synthesized by hydrothermal (or solvothermal) methods which make use of conventional electric heating, and generally require a long synthesis time. In recent years, however, new synthesis procedures including electrochemical, mechanochemical, sonochemical and microwave-assisted methods have been applied to the preparation of metal-organic frameworks.¹⁵ Compared to conventional solvothermal synthesis, microwave-assisted methods can sharply reduce the overall processing time, which, combined with the high yield usually obtained, significantly rises the energy efficiency of industrial production processes.^{15,16}

We report herein on a new, easy and rapid microwave-assisted method to synthesize the heterobimetallic sodium-cadmium organic framework $[\text{Cd}_3\text{Na}_6(\text{BTC})_4(\text{H}_2\text{O})_{12}]\cdot\text{H}_2\text{O}$ and, moreover, we show that the microwave-assisted procedure improves gas adsorption properties of the obtained material. With a view to increase knowledge about the prospective use of alkali metal-organic frameworks as carbon dioxide adsorbents for CCS, the gas adsorption properties of this newly prepared MOF were also investigated. Regenerability and multicycle stability were evaluated by cyclical CO_2 adsorption-desorption measurements. The results are discussed in the broader context of relevant data reported in the literature for CO_2 adsorption on both, other MOFs and cation-exchanged zeolites.

Experimental section

Synthesis of $[\text{Cd}_3\text{Na}_6(\text{BTC})_4(\text{H}_2\text{O})_{12}]\cdot\text{H}_2\text{O}$

The sodium-cadmium MOF described herein was synthesized following a similar procedure to that described by Fu et al.,¹⁴

except that we used microwave heating of the reaction mixture instead of the conventional electric heating used by those authors. The reaction mixture consisted of 4.0 mmol of cadmium acetate dihydrate (Sigma-Aldrich, 98%), 16 mmol of trimesic acid (Aldrich, 95%), 48 mmol of sodium hydroxide (Panreac, 97%), 14 ml of *N,N'*-dimethylacetamide (DMA) (Sigma-Aldrich, 99.5%) and 18 ml of deionized water, which were mixed inside the 50 ml Teflon vial of the autoclave. Once this mixture was homogenized, the autoclave was placed inside a microwave oven (Start D, Milestone, maximum power 350 W) and kept at 403 K for 1 h. The obtained solid was successively washed with DMA and deionized water and dried at room temperature in air. The prepared sample was stored under ambient conditions (average relative humidity of about 50% and room temperature). For comparison, a sample of $[\text{Cd}_3\text{Na}_6(\text{BTC})_4(\text{H}_2\text{O})_{12}]\cdot\text{H}_2\text{O}$ was also synthesized following the procedure previously reported by Fu et al.,¹⁴ which involved using conventional electric heating, instead of microwave heating, and keeping the reaction mixture for 5 days at 403 K. Hereafter, the sample prepared using conventional electric heating will be termed (Na,Cd)-MOF(CEH) to differentiate it from the sample prepared under microwave heating that will be termed (Na,Cd)-MOF.

Characterization

Powder X-ray diffraction data were collected using $\text{CuK}\alpha$ radiation on a Siemens D5000 diffractometer. Particle morphology was analyzed by scanning electron microscopy using a Hitachi S-3400N microscope operated at 15 kV. For textural characterization, N_2 adsorption-desorption isotherms at 77 K were measured in a volumetric analyzer (ASAP 2020HD, Micromeritics) equipped with a turbo molecular vacuum pump and three pressure transducers, allowing accurate measurements between 10^{-6} and 1.2 bar. The samples were previously outgassed under a dynamic vacuum (ca. 10^{-5} mbar) at 473 K overnight. Ultrahigh purity N_2 (99.992 %) was supplied by Air Products. The Brunauer-Emmett-Teller (BET) theory was used

to calculate the specific surface area, and the micropore size was analyzed using the Horvath-Kawazoe method, assuming cylindrical pore geometry.¹⁷

Variable temperature IR spectroscopy

For infrared spectroscopy, thin self-supported wafers of the MOF samples were prepared and activated (outgassed) in a dynamic vacuum (residual pressure smaller than 10^{-4} mbar) at 553 K for 8 h inside a 2000-A-C AABSPEC cell that allowed us to perform: (i) in situ sample activation, (ii) gas dosage and (iii) variable-temperature IR (VTIR) spectroscopy of adsorbed carbon dioxide while simultaneously recording temperature and equilibrium pressure. A K-thermocouple (in contact with the sample wafer) connected to a digital thermometer (TEMP, XS Instruments) and a capacitance pressure gauge (MKS, Baratron) were used for that purpose; the precision of the measurements was about ± 2 K and $\pm 2 \times 10^{-2}$ mbar for temperature and pressure, respectively.

After thermal activation of the sample wafer, the cell was dosed with carbon dioxide and closed, and transmission FTIR spectra were recorded while simultaneously registering the temperature and the gas equilibrium pressure inside the cell. In order to check reproducibility, and also to improve accuracy, the cell was then outgassed and dosed again with CO_2 , and a new series of variable temperature IR spectra was recorded. Transmission FTIR spectra were collected, at 3 cm^{-1} resolution, on a Bruker Vertex 80v spectrometer equipped with an MCT cryodetector.

From the integrated absorbance of the characteristic IR absorption band of adsorbed CO_2 in a series of spectra taken over a temperature range while simultaneously recording temperature (T) and equilibrium pressure (p) inside a closed IR cell, the standard adsorption enthalpy (ΔH^0) involved in the carbon dioxide adsorption process can be determined following the variable-temperature IR (VTIR) method described in detail elsewhere.^{18,19} In essence, at any given temperature, the integrated intensity, A , of the IR absorption band of adsorbed CO_2 should be proportional to the surface coverage, θ , thus giving information on the activity (in the thermodynamic sense) of both the adsorbed species and the empty adsorption sites, $1 - \theta$. Simultaneously, the equilibrium pressure provides information on the activity of the gas phase. Hence, the corresponding adsorption equilibrium constant, K , at that temperature, can be determined, and the variation of K with temperature yields the corresponding value of adsorption enthalpy. Assuming Langmuir-type adsorption, we have:

$$\theta = A/A_M = K(T)p / [1 + K(T)p] \quad (1)$$

where A_M is the integrated intensity corresponding to full coverage ($\theta = 1$). Combination of Equation (1) with the well known van't Hoff Equation (2) leads to Equation (3) below:

$$K(T) = \exp(-\Delta H^0/RT)\exp(\Delta S^0/R) \quad (2)$$

$$\ln[A/(A_M - A)p] = (-\Delta H^0/RT) + (\Delta S^0/R), \quad (3)$$

from which the desired ΔH^0 value can be obtained.

Carbon dioxide adsorption

CO_2 adsorption-desorption isotherms were measured, at 273 and 298 K, using a Micromeritics Tristar 3020 instrument working in the pressure range of 10^{-4} to 1.2 bar. The analyzer was equipped with a pressure transducer having a capacity of

1.33 bar (accuracy within 0.15 % of reading value). The sample outgassing conditions before the adsorption measurements were as stated above. During each measurement run, temperature was kept constant (within ± 0.5 K) using a thermostatic circulating-oil bath. The isosteric heat of adsorption was determined from the obtained equilibrium isotherms using the Clausius-Clapeyron equation. Ultrahigh purity CO_2 (i.e., 99.995) was supplied by Air Products.

Regenerability and multicycle stability of the (Na,Cd)-MOF sample was investigated using a thermoanalyzer instrument-SDT 2960 (TA Instruments). Approximately 10 mg of the sample was heated from 298 to 373 K at 5 K min^{-1} under nitrogen at a flow rate of 100 ml min^{-1} . The sample was then held at 373 K for 90 min, after which it was cooled to 308 K. Then the gas input was switched from N_2 to CO_2 and held at 308 K for 60 min. The CO_2 adsorption capacity was determined from the weight change of the sample after saturation with CO_2 . For multicycle stability evaluation the above described procedure was repeated 15 times.

Results and discussion

The synthesis procedure for the microwave-assisted preparation of the sodium-cadmium MOF was similar to that reported previously by Fu et al.,¹⁴ the main differences being the type of heating (microwave instead of electric) and the synthesis time (1 h instead of 5 days). A high yield (of about 92% in $\text{Cd}(\text{CH}_3\text{COO})_2 \cdot \text{H}_2\text{O}$) was obtained, which was (approximately) the same one attained when using conventional electric heating. The powder X-ray diffractogram of the obtained product showed good crystallinity, and was in good agreement with the powder diffraction pattern reported by Fu et al.,¹⁴ as shown in Fig. 2, where the diffractogram of the sodium-cadmium MOF synthesized using conventional electric heating is also shown for comparison. The obtained (Na,Cd)-MOF does not require any post-synthesis treatment (such as subsequent solvent exchange) and can be stored under ambient conditions (average relative humidity of 50% and room temperature) over a long time period (see later). These are important facts regarding potential industrial production and application.

Thermal stability was assessed by thermogravimetric analysis (TGA) in air (Fig. S1, supplementary information). The TGA curve was found to be very similar to that reported by Fu et al.¹⁴ The first step seen in the temperature range of 323 to 423 K corresponds to the loss of both, free and coordinated water molecules. This is followed by a plateau covering the range of 423-643 K, and an abrupt weight loss starting at the latter temperature (due to the vaporization of the organic linker). Hence, this TGA pattern provides clear evidence of structural stability up to ca. 643 K.

Fig. 3 shows scanning electron micrographs of the as-synthesized MOF samples prepared by using both microwave heating (a,b) and electric heating (c,d). Both materials show crystals having an (approximately) octahedral shape with an average size of approximately 3.5 and 7 μm , respectively, thus suggesting that the former has a larger external surface area. The observed difference in particle size can be explained in terms of nucleation and growth kinetics. At a difference with convection heating in an electric oven, microwave heating provides a much more uniform temperature across the synthesis mixture contained in the autoclave vase, thus speeding up nucleation rate of the solid reaction product and inhibiting crystal growth. This is in agreement with recent reports from several authors,²⁰⁻²⁴ who showed that microwave heating leads

to a significantly smaller particle size than convection heating in the synthesis of several other metal-organic frameworks.

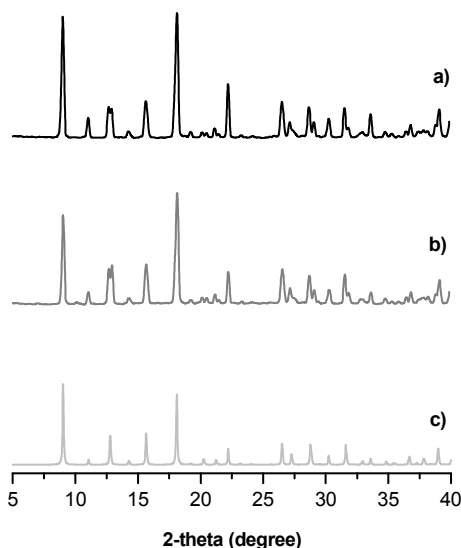


Fig. 2 Powder X-ray diffraction patterns (Cu-K α radiation) of a) (Na,Cd)-MOF and b) (Na,Cd)-MOF(CEH); c) simulated diffractogram obtained from the crystallographic data of Fu et al.¹⁴

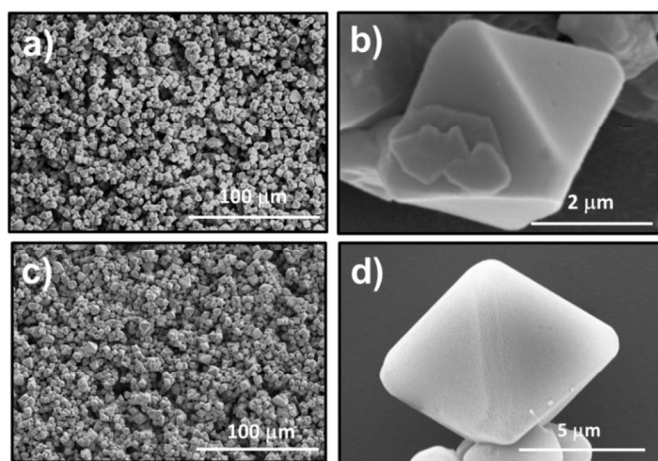


Fig. 3 SEM micrographs of the sodium-cadmium MOFs synthesized by: a-b) microwave and c-d) conventional electric heating.

Textural characterization by means of the corresponding nitrogen adsorption isotherms at 77 K (Fig. S2) showed that both MOF samples are highly microporous materials, exhibiting reversible type I isotherms with no hysteresis. The steep rise of the adsorption isotherms at relative pressure below 0.1, and the observed slow adsorption of nitrogen, are characteristic of a pore network comprised (mainly) of micropores having small diameter. This was further confirmed by Hovarth-Kawazoe analysis which rendered an average pore size of ca. 0.8 nm in both cases, which is in good agreement with the pore aperture reported by Fu et al.¹⁴ The BET specific

surface area resulted to be 526 m² g⁻¹ for the sodium-cadmium MOF sample obtained by microwave heating, and 418 m² g⁻¹ for the sample obtained under conventional electric heating. Fu et al.¹⁴ report for their (Na,Cd)-MOF (prepared by conventional electric heating) a specific surface area of 473 m² g⁻¹ (determined from the corresponding nitrogen adsorption isotherm at 77 K). This value is about 10% larger than that of our (Na,Cd)-MOF(CEH) sample, but still significantly smaller than that of our (Na,Cd)-MOF. As already mentioned above, the smaller particle size of the (Na,Cd)-MOF synthesized by microwave heating could contribute to a correspondingly larger surface area.

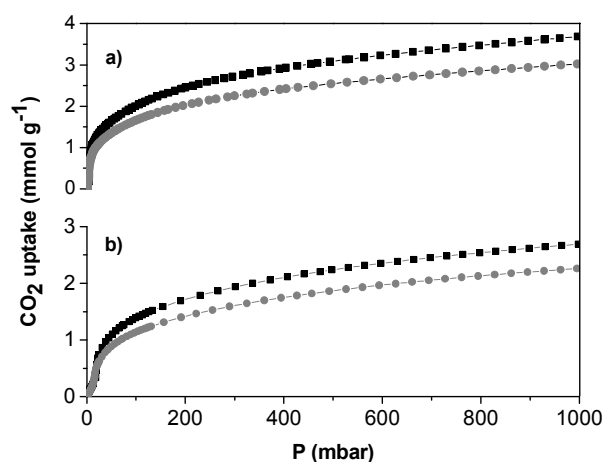


Fig. 4 Carbon dioxide adsorption isotherms of the (Na,Cd)-MOF (black) and (Na,Cd)-MOF(CEH) (gray) at: a) 273 and b) 298 K.

The CO₂ adsorption isotherms of the two MOF samples collected at two different temperatures, 273 and 298 K, are depicted in Fig. 4; they both show a steep rise of CO₂ uptake at low pressure, which is characteristic of porous materials having binding sites that show a relatively high affinity for CO₂ (such as coordinatively unsaturated metal cations). At 298 K and 1 bar, the sample prepared under microwave heating shows a carbon dioxide uptake of 2.71 mmol g⁻¹, which is higher than the value of 2.25 mmol g⁻¹ shown by the sample prepared using conventional electric heating. Table 1, which collects relevant literature data,^{9,13,25-49} shows that the CO₂ uptake of the (Na,Cd)-MOF ranks among the highest values reported so far for alkali metal-organic frameworks and is similar to those of several other MOFs proposed as potential CO₂ sorbents; although lower than the uptake shown by Mg-DOBDC, HKUST-1 and other MOFs containing copper or cobalt, as well as the zeolites Na-A and Na-X. It is worthwhile pointing out that for stationary applications, such as postcombustion CO₂ capture from power plants, the volumetric capacity, which takes into account the density of the adsorbent can be a better indicator of performance than the gravimetric capacity; because increased volumetric capacity can lead to a reduced size of the gas adsorption towers, which facilitates heating efficiency during the adsorbent regeneration step.^{50,51} Taking into account the relatively high density of the (Na,Cd)-MOF (D= 1.921 g cm⁻³, according to crystallographic data),¹⁴ the volumetric capacity of this MOF, at 298 K and 1 bar, results to be 5.2 mmol cm⁻³. This value is higher than that of the Na-A zeolite (4.7 mmol cm⁻³) and closer (or even higher) to those of some

Table 1. Adsorption heat and uptake capacity for carbon dioxide adsorbed on several metal-organic frameworks and zeolites

Adsorbent	$-\Delta H^0$ (kJ mol ⁻¹) [§]	Method ^a	CO ₂ uptake (mmol g ⁻¹) [*]	Ref.
MOFs				
(Na,Cd)-MOF	42.0 (35)	Q _{st}	2.71	This work
Mg-MOF-74	47.0	VTIR	-	25
Mg-DOBDC ^a	47.0 (25)	Q _{st}	8.08	26
[Na ₂ (SBA)] or CYCU-6 ^b	-	-	1.33	13
[Ca(SBA)]·0.45H ₂ O or CYCU-1 ^b	28.0 (18)	Q _{st}	1.37	27
[Sr(SBA)]·0.20H ₂ O or CYCU-2 ^b	-	-	1.17	27
CD-MOF-2 ^c	-	-	2.36	28
[(Li ⁺)-(C ₆ H ₄ NO ₂ ⁻)]·0.5DMF	35.0 (25)	Q _{st}	0.92	29
{Mg(DHT)(DMF) ₂ } ^d	-	-	2.71 (195 K)	30
Mg-MOF-1 ^e	-	-	0.63	31
Mg(HCOO) ₂	-	-	1.70	32
SNU-25 ^f	-	-	1.49	33
{[Ca(ptaH)(H ₂ O)]·6H ₂ O} ^g	-	-	0.76	34
[Ca(SDB)]·H ₂ O ^h	31.0 (28)	Q _{st}	0.99	35
SNU-100-Li ⁱ	35.7 (34)	Q _{st}	3.47	36
SNU-100-Mg ⁱ	36.3 (35)	Q _{st}	3.43	36
SNU-100-Ca ⁱ	37.4 (36)	Q _{st}	3.43	36
Co ₂ (ad) ₂ (CO ₂ CH ₃) ₂ or bio-MOF-1 ^j	45.0 (30)	Q _{st}	4.06	37
Co-MOF-74	51.0 (30)	Q _{st}	6.50	24
Cu ₃ (BHB) or UTSA-20 ^k	-	-	5.10	38
Cu(Me-4py-trz-ia) ^l	30.0 (30)	Q _{st}	6.09	39
Cu ₃ (TDPAT)(H ₂ O) ₃ ^m	42.2 (23)	Q _{st}	5.90	40
HKUST-1	-	-	5.54	9
	29.8 (29)	Q _{st}	2.94 (315 K)	41
MOF-5	16.5	Q _{st}	1.12	21
ZEOLITES				
Li-ZSM-5	58.9	Q _{st}	2.50	42
Na-A	42.0-44.0 ⁿ	VTIR	-	43
	30.0 (30)	Q _{st}	3.10	44
Na-ZK-4	42.0 (30)	Q _{st}	3.6	45
Na,K-ZK-4	-	-	3.8-3.0 (273 K)	45
Na-X	49.1 (36)	Q _{st}	5.4	46
	49.0 (40)	Q _{st}	5.6	44
Na-FER	49.8-58.8 ⁿ	Q _{st}	1.75-0.94 ^o	47
Na-ZSM-5	50.0 (30)	Q _{st}	1.91	46
	46.3	Q _{st}	2.4	42
K-FER	41-51 ⁿ	Q _{st}	-	3,48
	44.6-51.8 ⁿ	Q _{st}	1.75-0.84 ^o	47
K-L	42.5	VTIR	-	49
K-ZSM-5	36.0	Q _{st}	2.2	42
Rb-ZSM-5	34.9	Q _{st}	1.9	42
Cs-ZSM-5	33.0	Q _{st}	1.4	42

[§] Values extrapolated at zero coverage are shown, and (when reported in the literature) values corresponding to a large CO₂ uptake are given between brackets; ^{*}P= 1 bar; T= 298 K; ^a DOBDC: 2,5-dioxido-1,4-benzenedicarboxylate; ^b Prepared from NaOH and 4,4'-sulfonyldibenzoic acid (H₂SBA); ^c Prepared from RbOH and γ -cyclodextrin; ^d DHT: 2,5-dihydroxyterphthalate; ^e [Mg(3,5-PDC)(H₂O)] where 3,5-PDC is 3,5-pyridine dicarboxylic acid; ^f [Mg(TCPBDA)] where TCPBDA is N,N,N',N'-tetrakis(4-carboxyphenyl)-biphenyl-4,4'-diamine; ^g ptaH₃; ^h tris-{2-(4-carboxyphenoxy)ethyl}amine; ⁱ SDB: 4,4'-sulfonyldibenzoate; ^j SNU-100: [Zn₃(TCPT)₂(HCOO)][(NH₂(CH₃)₂)] exchanged with Li⁺, Mg²⁺ and Ca²⁺ ions; ^k ad: adeninate; ^l BHB: 3,3',3'',5,5',5''-benzene-1,3,5-triylhexabenzic acid; ^m Me-4pyz-trz-ia: 5-(3-methyl-5-(pyridine-4-yl)-(4H-1,2,4-triazol-4-yl)isophthalate); ⁿ H₆TDPAT: 2,4,6-tris(3,5-dicarboxylphenylamino)-1,3,5-triazine; ^o Depending on the adsorption site; ^p Depending on the Si/Al ratio.

high performing metal-organic frameworks, such as Bio-MOF-11³⁷ (5.0 mmol cm⁻³), UTSA-20³⁸ (4.6 mmol cm⁻³), Cu(Me-4py-trz-ia)³⁹ (5.6 mmol cm⁻³), Cu₃(TDPAT)(H₂O)₃⁴⁰ (4.6 mmol cm⁻³) or HKUST-1^{9,52} (4.5 mmol cm⁻³). Note also that the (Na,Cd)-MOF has the additional advantage, compared to other MOFs, that it can be used as-synthesized without subsequent solvent exchange, and also that thermal activation at 373 K is enough to achieve maximum adsorption capacity. Fig. 5 shows the isosteric heat of adsorption, Q_{st} , of CO₂ (as a function of uptake) derived from the corresponding adsorption isotherms at 273 and 298 K shown in Fig. 4 for the MOF synthesized under microwave heating. Extrapolation of the curve in Fig. 5 to zero coverage gives the value of $Q_{st} = 42$ kJ mol⁻¹, which decreases to about 35 kJ mol⁻¹ when the CO₂ uptake reaches 1.5 (and remains nearly constant for higher uptake values). The observed higher value of Q_{st} at low coverage should correspond to direct interaction between CO₂ molecules and coordinatively unsaturated Na⁺ ions (see below), which according to crystallographic data¹⁴ occupy different adsorption sites along the channel system. Note also that the relatively high Q_{st} value (35 kJ mol⁻¹) observed at high CO₂ loadings (which is close to the isosteric heat of adsorption of carbon dioxide on some other MOFs) is probably due to adsorbate-framework and adsorbate-adsorbate interactions, which are magnified by the narrow diameter of the sodium-cadmium MOF channels.

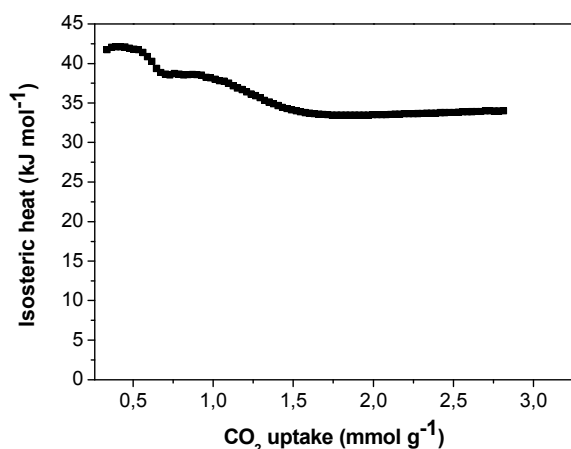


Fig. 5 Isosteric heat of adsorption of carbon dioxide on (Na,Cd)-MOF.

Direct interaction between adsorbed carbon dioxide and coordinatively unsaturated sodium cations was corroborated by variable-temperature IR spectroscopy. Representative variable-temperature FT-IR spectra (in the CO₂ asymmetric stretching region) of carbon dioxide adsorbed on the (Na,Cd)-MOF are depicted in Fig. 6a. A broad IR absorption band is seen, centred at 2344 cm⁻¹, which is assigned to the CO₂ asymmetric stretching vibration (ν_3 mode) of carbon dioxide interacting with the coordinatively unsaturated sodium cations. The corresponding value for the free CO₂ molecule is 2349.3 cm⁻¹. However, carbon dioxide confined inside the pores of silicalite (a purely siliceous zeolite) is known to show the ν_3 mode at 2341 cm⁻¹, as a result of the confinement effect.⁵³ Taking this value as the reference, the spectra in Fig. 6a show a

hypsochromic shift of 3 cm⁻¹. From the integrated absorbance of spectra obtained in two independent series of VTIR measurements, the van't Hoff plot depicted in Fig. 6b was obtained, applying Eq. 3. From that linear plot the corresponding value of standard adsorption enthalpy for CO₂ resulted to be $\Delta H^0 = -42$ kJ mol⁻¹; the estimated error limit is ± 1 kJ mol⁻¹. This ΔH^0 value is in good agreement with that of Q_{st} extrapolated to zero coverage (reported above). To conclude this section, the IR spectroscopic results reported herein can be compared with corresponding data reported in the literature for Na-exchanged zeolites (since no similar data seem to be available for sodium-containing MOFs). For CO₂ adsorbed in Na-ZSM-5, Bonelli et al.⁵⁴ report the ν_3 value of 2356 cm⁻¹ and an adsorption heat of 48 kJ mol⁻¹ (extrapolated to zero coverage); while for CO₂ in Na-ZK-4 Cheung et al.⁴⁵ give $\nu_3 = 2360$ cm⁻¹ and an adsorption heat of 42 kJ mol⁻¹. The smaller values found herein for the investigated (Na,Cd)-MOF suggest a weaker (local) interaction of the CO₂ molecule with the Na⁺ cation. However, analysis of fine details cannot be done at this stage, because it was shown that for CO₂ adsorbed on both, MOFs and zeolites alike, at least one half of the gas-solid interaction energy comes from long range dispersion interactions,^{25,55,56} and the actual value of ΔH^0 depends on a complex interplay of electrostatic and dispersion forces.

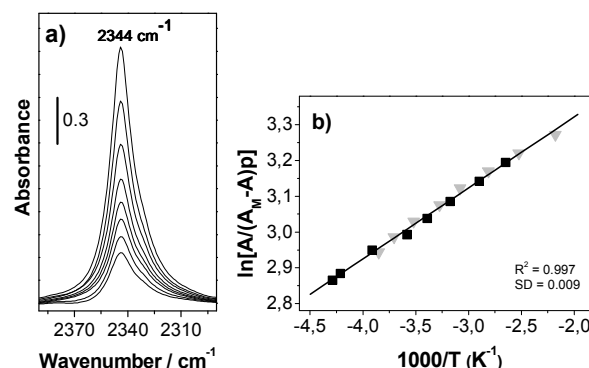


Fig. 6 a) Representative VTIR spectra (MOF blank subtracted) of CO₂ adsorbed on the (Na,Cd)-MOF. From top to bottom temperature goes from 308 to 347 K, and equilibrium pressure from 5.40 to 5.67 mbar. b) Plot of the left-hand side of Eq. (3) against the reciprocal of the temperature. R, linear regression coefficient; SD, standard deviation. Squares and triangles stand for two different series of IR spectroscopic measurements.

Adsorption selectivity, of carbon dioxide versus nitrogen, referred to post-combustion flue gas that (besides other minor components) usually contains CO₂ and N₂ at a partial pressure of about 0.15 and 0.75 bar, respectively, is commonly assessed from single-component gas adsorption isotherms (at 298 K) by using the selectivity factor, S , expressed as:^{2,11}

$$S = \frac{q_1 p_2}{q_2 p_1} \quad (4)$$

where q_i and p_i are the molar fraction and partial pressure, respectively, of component i . Note that single-component isotherms do not necessarily account for actual selectivity (mainly because competition for adsorption sites is neglected)

but binary isotherms are not usually reported in the literature, and the selectivity factor defined above is widely used to rank (as a first approximation) different adsorbents for carbon dioxide capture by physical adsorption. Adsorption isotherms of N_2 and CO_2 on (Na,Cd)-MOF are depicted in Fig. 7. From these isotherms the value of $S = 50$ was obtained for the selectivity of CO_2 versus nitrogen; this value is higher than those reported for Mg-MOF-74 (44.4) and other MOFs considered good candidates for CO_2 capture from industrial flue gases, such as Ni-MOF-74 (30.0), Cu-TDPAT (34.2) or HKUST-1 (34.4), and also higher to those shown by approximately one half of the 56 MOFs compiled in a recent list.¹¹

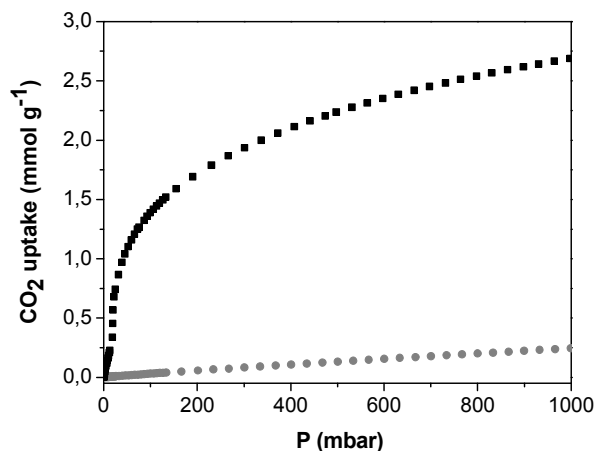


Fig. 7 Carbon dioxide (black squares) and nitrogen (grey circles) adsorption isotherms at 298 K on (Na,Cd)-MOF.

One of the main drawbacks for industrial scale applications of MOFs is their low thermal and chemical stability when exposed to air and moisture.^{6,57} This instability limits the industrial implementation of a great number of metal-organic frameworks. Besides that, although the CO_2 uptake capacity under dry conditions is an important criterion for identifying suitable sorbents for CO_2 capture and storage, tolerance to the presence of moisture in the feed and retention of the uptake capacity when the sorbent is regenerated after exposure to humid conditions are very important factors when choosing a candidate for further development.⁵⁸ To check stability upon exposure to air and water vapour, a (Na,Cd)-MOF sample was stored during 3 months at ambient conditions (room temperature and an average humidity of 50%) followed by storing for increasing time periods (1 hour, 1 day and 1 week) at room temperature and 95% humidity. The nearly identical powder X-ray diffraction patterns (Fig. S3) shown by the sample after each treatment testify to sample stability. The hydrated sample was then activated by outgassing at 373 K and its carbon dioxide adsorption capacity determined (Fig. S3, inset); the same CO_2 capacity as the pristine material was obtained demonstrating that, even after extended exposure to humid atmosphere, the sodium metal-organic framework is stable and exhibits the same ability to capture carbon dioxide after regeneration. Similarly, (Na,Cd)-MOF(CEH) was found to be also stable in humid air (Fig. S4).

Also the cyclic and thermal stability of MOFs during adsorption-desorption is very important when connected to

practical application. To ensure the regenerability and the recyclability of the materials, we further performed some regeneration and CO_2 adsorption cycling measurements using a combined temperature swing and nitrogen purge approach as described in the Experimental Section (last paragraph). Results are summarized in Fig. 8 where it can be observed that after 15 cycles the CO_2 adsorption capacity of Na-MOF was retained, testifying its stability.

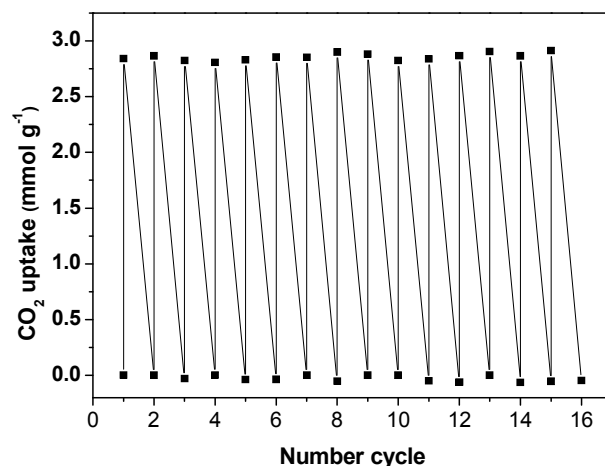


Fig. 8 CO_2 adsorption cycles for the (Na,Cd)-MOF (repetitive CO_2 adsorption at 308 K followed by desorption at 373 K under a N_2 purge).

Conclusions

In summary, a novel, easy and fast microwave-assisted method has been developed to synthesize a sodium-cadmium metal-organic framework having coordinatively unsaturated Na^+ sites. The (Na,Cd)-MOF thus prepared can be used as-synthesized, without any subsequent solvent exchange, and shows permanent porosity after solvent removal, and long-term stability even in a humid atmosphere. CO_2 adsorption capacity, at 298 K and 1 bar (which was shown to be higher than that of a sample of the same MOF synthesized by using conventional electric heating) ranks among the values shown by some of the most prospective metal-organic frameworks for CO_2 capture from the flue gas of post-combustion power stations. The newly prepared (Na,Cd)-MOF displays a high selectivity for the adsorption of carbon dioxide over nitrogen; and, unlike several other metal-organic frameworks, it can be regenerated under soft conditions and shows good recyclability during adsorption-desorption CO_2 cycles.

Acknowledgments

The Spanish Ministerio de Economía y Competitividad (MINECO) and the European Funds for Regional Development (FEDER) are gratefully acknowledged for financial support through Project CTQ2013-47461-R. Financial support from “Programa Pont la Caixa per a grups de recerca de la UIB” is also acknowledged. C.P. acknowledges the Spanish Ministerio de Educación y Ciencia (pre-doctoral fellowship).

References

1. R. Quadrelli and S. Peterson, *Energy Policy*, 2007, **35**, 5938–5952.

2. K. Sumida, D. L. Rogow, J. A. Mason, T. M. McDonald, E. D. Bloch, Z. R. Herm, T.-H. Bae and J. R. Long, *Chem. Rev.*, 2012, **112**, 724–781.
3. L. Grajciar, J. Čejka, A. Zukal, C. Otero Areán, G. Turnes Palomino and P. Nachtigall, *ChemSusChem*, 2012, **5**, 2011–2022.
4. J.-R. Li, Y. Ma, M. C. McCarthy, J. Sculley, J. Yu, H.-K. Jeong, P. B. Balbuena and H.-C. Zhou, *Coord. Chem. Rev.*, 2011, **255**, 1791–1823.
5. *IPCC Special Report on Carbon Dioxide Capture and Storage*, 2005.
6. J. Liu, P. K. Thallapally, B. P. McGrail, D. R. Brown and J. Liu, *Chem. Soc. Rev.*, 2012, **41**, 2308–2322.
7. S. H. Jung, N. A. Khan and Z. Hasan, *CrystEngComm*, 2012, **14**, 7099–7109.
8. H. Furukawa, K. E. Cordova, M. O’Keeffe and O. M. Yaghi, *Science*, 2013, **341**, 1230444–1–1230444–12.
9. Z. Zhang, Y. Zhao, Q. Gong, Z. Li and J. Li, *Chem. Commun.*, 2013, **49**, 653–661.
10. B. Li, H. Wang and B. Chen, *Chem. Asian J.*, 2014, **9**, 1474–1498.
11. Z. Zhang, Z.-Z. Yao, S. Xiang and B. Chen, *Energy Environ. Sci.*, 2014, **7**, 2868–2899.
12. D. Banerjee and J. B. Parise, *Cryst. Growth Des.*, 2011, **11**, 4704–4720.
13. D. S. Raja, J.-H. Luo, C.-Y. Wu, Y.-J. Cheng, C.-T. Yeh, Y.-T. Chen, S.-H. Lo, Y.-L. Lai and C.-H. Lin, *Cryst. Growth Des.*, 2013, **13**, 3785–3793.
14. Y. Fu, J. Su, Z. Zou, S. Yang, G. Li, F. Liao and J. Lin, *Cryst. Growth Des.*, 2011, **11**, 3529–3535.
15. C. Dey, T. Kundu, B. P. Biswal, A. Mallick and R. Banerjee, *Acta Crystallogr. B. Struct. Sci. Cryst. Eng. Mater.*, 2014, **70**, 3–10.
16. J. Klinowski, F. A. A. Paz, P. Silva and J. Rocha, *Dalton Trans.*, 2011, **40**, 321–330.
17. G. Horvath and K. Kawazoe, *J. Chem. Eng. Japan*, 1983, **16**, 470–475.
18. E. Garrone and C. Otero Areán, *Chem. Soc. Rev.*, 2005, **34**, 846–857.
19. C. Otero Areán, O. V. Manoilova, G. Turnes Palomino, M. Rodríguez Delgado, A. A. Tsyganenko, B. Bonelli and E. Garrone, *Phys. Chem. Chem. Phys.*, 2002, **4**, 5713–5715.
20. S. H. Jung, J.-H. Lee, J. W. Yoon, C. Serre, G. Férey and J.-S. Chang, *Adv. Mater.*, 2007, **19**, 121–124.
21. J.-S. Choi, W.-J. Son, J. Kim and W.-S. Ahn, *Microporous Mesoporous Mater.*, 2008, **116**, 727–731.
22. C.-M. Lu, J. Liu, K. Xiao and A. T. Harris, *Chem. Eng. J.*, 2010, **156**, 465–470.
23. E. Haque, N. A. Khan, J. H. Park and S. H. Jung, *Chem. Eur. J.*, 2010, **16**, 1046–1052.
24. H.-Y. Cho, D.-A. Yang, J. Kim, S.-Y. Jeong and W.-S. Ahn, *Catal. Today*, 2012, **185**, 35–40.
25. L. Valenzano, B. Civalleri, S. Chavan, G. T. Palomino, C. O. Arean and S. Bordiga, *J. Phys. Chem. C*, 2010, **114**, 11185–11191.
26. S. R. Caskey, A. G. Wong-Foy and A. J. Matzger, *J. Am. Chem. Soc.*, 2008, **130**, 10870–10871.
27. C.-T. Yeh, W.-C. Lin, S.-H. Lo, C.-C. Kao, C.-H. Lin and C.-C. Yang, *CrystEngComm*, 2012, **14**, 1219–1222.
28. R. S. Forgan, R. A. Smaldone, J. J. Gassensmith, H. Furukawa, D. B. Cordes, Q. Li, C. E. Wilmer, Y. Y. Botros, R. Q. Snurr, A. M. Z. Slawin and J. F. Stoddart, *J. Am. Chem. Soc.*, 2012, **134**, 406–417.
29. B. F. Abrahams, M. J. Grannas, T. A. Hudson and R. Robson, *Angew. Chem. Int. Ed.*, 2010, **49**, 1087–1089.
30. K. Jayaramulu, P. Kanoo, S. J. George and T. K. Maji, *Chem. Commun.*, 2010, **46**, 7906–7908.
31. A. Mallick, S. Saha, P. Pachfule, S. Roy and R. Banerjee, *J. Mater. Chem.*, 2010, **20**, 9073–9080.
32. D. G. Samsonenko, H. Kim, Y. Sun, G.-H. Kim, H.-S. Lee and K. Kim, *Chem. Asian J.*, 2007, **2**, 484–488.
33. Y. E. Cheon, J. Park and M. P. Suh, *Chem. Commun.*, 2009, 5436–5438.
34. S. Neogi, J. A. R. Navarro and P. K. Bharadwaj, *Cryst. Growth Des.*, 2008, **8**, 1554–1558.
35. D. Banerjee, Z. Zhang, A. M. Plonka, J. Li and J. B. Parise, *Cryst. Growth Des.*, 2012, **12**, 2162–2165.
36. H. J. Park and M. P. Suh, *Chem. Sci.*, 2013, **4**, 685–690.
37. J. An, S. J. Geib and N. L. Rosi, *J. Am. Chem. Soc.*, 2010, **132**, 38–39.
38. Z. Guo, H. Wu, G. Srinivas, Y. Zhou, S. Xiang, Z. Chen, Y. Yang, W. Zhou, M. O’Keeffe and B. Chen, *Angew. Chem. Int. Ed.*, 2011, **50**, 3178–3181.
39. D. Lässig, J. Lincke, J. Moellmer, C. Reichenbach, A. Moeller, R. Gläser, G. Kalies, K. A. Cychosz, M. Thommes, R. Staudt and H. Krautscheid, *Angew. Chem. Int. Ed.*, 2011, **50**, 10344–10348.
40. B. Li, Z. Zhang, Y. Li, K. Yao, Y. Zhu, Z. Deng, F. Yang, X. Zhou, G. Li, H. Wu, N. Nijem, Y. J. Chabal, Z. Lai, Y. Han, Z. Shi, S. Feng and J. Li, *Angew. Chem. Int. Ed.*, 2012, **51**, 1412–1415.
41. C. R. Wade and M. Dinca, *Dalton Trans.*, 2012, **41**, 7931–7938.
42. T. Yamazaki, M. Katoh, S. Ozawa and Y. Ogino, *Mol. Phys.*, 1993, **80**, 313–324.
43. A. Zukal, C. O. Arean, M. R. Delgado, P. Nachtigall, A. Pulido, J. Mayerová and J. Čejka, *Microporous Mesoporous Mater.*, 2011, **146**, 97–105.
44. T.-H. Bae, M. R. Hudson, J. A. Mason, W. L. Queen, J. J. Dutton, K. Sumida, K. J. Micklash, S. S. Kaye, C. M. Brown and J. R. Long, *Energy Environ. Sci.*, 2013, **6**, 128–138.
45. O. Cheung, Z. Bacsik, P. Krokidas, A. Mace, A. Laaksonen and N. Hedin, *Langmuir*, 2014, **30**, 9682–9690.
46. J. A. Dunne, M. Rao, S. Sircar, R. J. Gorte and A. L. Myers, *Langmuir*, 1996, **12**, 5896–5904.
47. R. Bulánek, K. Frolich, E. Frýdová and P. Čičmanec, *Top. Catal.*, 2010, **53**, 1349–1360.
48. A. Zukal, A. Pulido, B. Gil, P. Nachtigall, O. Bludský, M. Rubes and J. Čejka, *Phys. Chem. Chem. Phys.*, 2010, **12**, 6413–6422.

Journal Name

49. C. O. Arean, G. F. Bibiloni and M. R. Delgado, *Appl. Surf. Sci.*, 2012, **259**, 367–370.
50. A. Das, M. Choucair, P. D. Southon, J. A. Mason, M. Zhao, C. J. Kepert, A. T. Harris and D. M. D'Alessandro, *Microporous Mesoporous Mater.*, 2013, **174**, 74–80.
51. J. A. Mason, K. Sumida, Z. R. Herm, R. Krishna and J. R. Long, *Energy Environ. Sci.*, 2011, **4**, 3030–3040.
52. S. S.-Y. Chui, S. M.-F. Lo, J. P. H. Charmant, A. G. Orpen and I. D. Williams, *Science*, 1999, **283**, 1148–1150.
53. B. Bonelli, B. Civalleri, B. Fubini, P. Ugliengo, C. Otero Arean and E. Garrone, *J. Phys. Chem. B*, 2000, **104**, 10978–10988.
54. B. Bonelli, B. Onida, B. Fubini, C. O. Arean and E. Garrone, *Langmuir*, 2000, **16**, 4976–4983.
55. A. Pulido, M. R. Delgado, O. Bludský, M. Rubeš, P. Nachtigall and C. O. Areán, *Energy Environ. Sci.*, 2009, **2**, 1187–1195.
56. P. Nachtigall, M. R. Delgado, D. Nachtigallova and C. O. Arean, *Phys. Chem. Chem. Phys.*, 2012, **14**, 1552–1569.
57. R. Sabouni, H. Kazemian and S. Rohani, *Microporous Mesoporous Mater.*, 2013, **175**, 85–91.
58. A. C. Kizzie, A. G. Wong-Foy and A. J. Matzger, *Langmuir*, 2011, **27**, 6368–6373.

Graphical abstract

A very stable sodium-cadmium metal-organic framework with high volumetric CO₂ adsorption capacity and selectivity has been prepared by a fast and easy microwave-assisted method.

